Journal of Alloys and Compounds 509 (2011) 9764–9769

Contents lists available at ScienceDirect

Journal of Alloys and Compounds

journal homepage: www.elsevier.com/locate/jallcom

A sol–gel route to nanocrystalline TiN coated cubic boron nitride particles

Malik Adeel Umer[a], Hee Sub Park[a,b], Dong Ju Lee[a], Ho Jin Ryu[c], Soon Hyung Hong[a,*]

[a] Department of Materials Science and Engineering, KAIST, 373-1 Kusung-Dong, Yusung-Gu, Daejeon 305-701, Republic of Korea
[b] Institute of Industrial Technology, ILJIN Diamond Co., Ltd., 614-2 Oryu-Ri, Daeso-Myun, Eumsung-Kun, Chungcheongbuk-Do, Republic of Korea
[c] Korea Atomic Energy Research Institute, 150 Deokjin-Dong, Yuseong-Gu, Daejeon 305-353, Republic of Korea

ARTICLE INFO

Article history:
Received 16 March 2011
Received in revised form 19 July 2011
Accepted 21 July 2011
Available online 28 July 2011

Keywords:
Nanostructured materials
Nitride materials
Sol–gel processes
Ceramics
Microstructure

ABSTRACT

For the purpose of increasing microstructural homogeneity and enhancing the reinforcement-matrix interfacial area, cubic Boron Nitride, cBN particles were coated by nanocrystalline TiN by a sol–gel route that required neither the need for pH adjustment nor the use of surfactants or additives. Uniform shells of amorphous titania having thicknesses in the nanometers scale were formed on the surface of the cBN particles by hydrolysis and condensation reactions of titanium (IV) isopropoxide. The amorphous coated cBN powder was nitrided to crystalline TiN coated cBN by treating in NH_3 gas at 900 °C. After nitridation the amorphous layer was completely converted to nanocrystalline TiN particles that uniformly covered the surface of cBN. Changes in the TiO_x coated layer thickness and the size of the TiN particles were investigated as a function of alkoxide content. TiO_2 nanoparticles were synthesized using the same reaction conditions, but without the presence of cBN. These nanoparticles were calcined in air at different temperatures (250–700 °C) and then nitrided at 900 °C. The nitridation behavior of TiO_2 nanoparticles was studied as a function of calcination temperature.

1. Introduction

Cubic boron nitride (cBN) is one of the hardest materials known to man and has excellent physical and chemical properties [1,2]. Because of these properties, the polycrystalline cubic boron nitride (PcBN) tools have been widely used for the machining of hard ferrous materials (hardened alloy steels, tool steels, cast iron, etc.), titanium based alloys, and nickel-based super-alloys [3–7]. In general, PcBN is fabricated by high temperature high pressure (HTHP) sintering process using cBN powder and binders composed of ceramic materials such as TiC, TiN, TiCN, and TiB_2 [8–10]. Due to the high melting point of the ceramic binders, the sintering mechanism of low grade PcBN tools is mainly the solid state type, involving a reaction of cBN with the binder to form intermetallic compounds at the cBN-binder interface. A homogenous microstructure having minimal cBN–cBN direct bonding is essential for an enhanced performance and reliability of the PcBN tools [11]. However, due to certain limitations of the powder processing techniques, it is impossible to avoid direct bonding between cBN particles. Previously, a TiN–TiB_2 coating was achieved on cBN particles with grain size less than 2 μm by a molten salts technique and was reported to have led to an increase in Vickers microhardness of the sintered compacts [12]. Although the sol–gel process is widely used for the synthesis of ceramics in the nanometers scale, binder-coated cBN (by the sol–gel process) has not been reported yet.

In this work, a sol–gel process has been employed to synthesize highly homogenous TiN coated cBN particles. The microstructure and the crystal structure of the composite powders were studied. The process consists of first coating the surface of cBN particles with an amorphous layer of TiO_x followed by nitridation to fine TiN coated cBN particles. Transmission electron microscopy (TEM) was used to study what effect changing alkoxide content has on the thickness of TiO_x coating layer and the diameter of TiN particles thus formed. X-ray diffraction (XRD) technique was used to calculate TiO_2 crystallite sizes and study the nitridation behavior of TiO_2 nanoparticles as a function of calcination temperature. Lattice parameter of coated TiN was compared with values of pure TiN.

2. Experimental procedures

2.1. Preparation of TiN coated cBN powders

The starting materials for the preparation of TiN coated cBN powders were cBN powder (Iljin Diamond Co., Ltd.), with a mean powder size of 0.5–1.0 μm; titanium (IV) isopropoxide, TTIP (Sigma–Aldrich) was selected as the precursor. The experimental procedure is shown in the form of a flow chart in Fig. 1.

cBN powder was treated in fuming concentrated sulphuric acid to which potassium nitrate was added. After washing and drying, cBN powder was further heated in air at 600 °C for 30 min. TiO_2 precursor solution was prepared by mixing titanium (IV) isopropoxide, TTIP with anhydrous ethanol for a concentration of 0.25 M TTIP. The solution was stirred for 30 min. Keeping the same concentration, the content of TTIP was varied, as shown in Table 1. 1 g of the surface treated cBN powder was ultrasonically suspended in 200 ml of anhydrous ethanol for 30 min, to which H_2O

* Corresponding author.
E-mail address: shhong@kaist.ac.kr (S.H. Hong).

0925-8388/$ – see front matter © 2011 Elsevier B.V. All rights reserved.
doi:10.1016/j.jallcom.2011.07.070

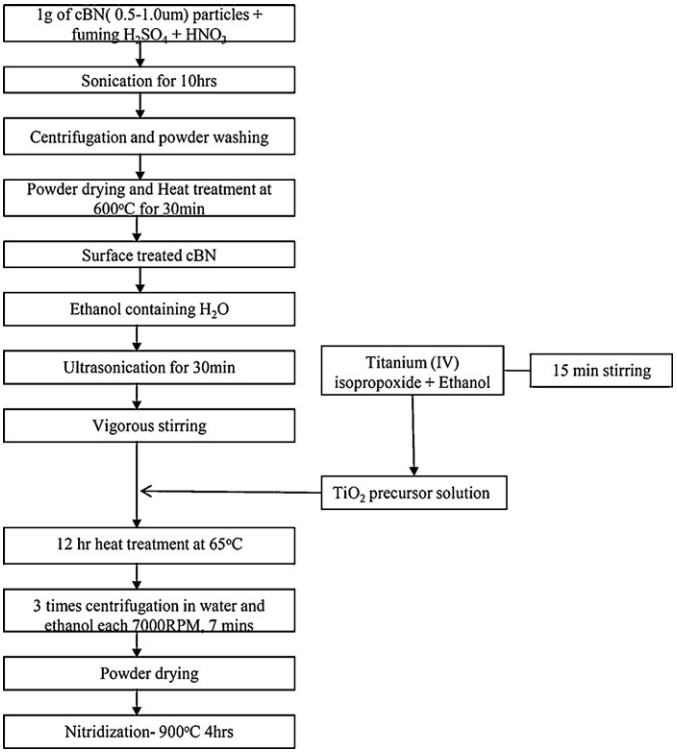

Fig. 1. Flowchart of the experimental procedure.

Table 1
The different amounts of the precursor used for the experiments.

S. No.	cBN/g	TTIP/ml	TTIP/mole	Volume % coated TiN
1	1	0.71	2.34×10^{-3}	10
2	1	1.42	4.68×10^{-3}	20
3	1	2.85	9.40×10^{-3}	40
4	1	4.30	0.014	60

had been added for a concentration of 1.6 M. The solution containing TTIP was added in a drop wise manner with the help of a micro tubing pump (Eyala MP-1000A), to a vigorously stirred suspension of cBN particles at a rate of 0.25 ml/min at a temperature of 25 °C. The titanium (IV) isopropoxide was hydrolyzed by the presence of water molecules in the solution. The resulting mixture was heated with the help of a closed heating mantle at 65 °C for 12 h. The titanium isopropoxide was hydrolyzed and polycondensed to form nanosized layers on the surface of the cBN particles. The final solution was centrifugated at 7000 rpm for 7 min and was washed several times with anhydrous ethanol and distilled water. The precipitates obtained were dried at 60 °C. TiO_x coated cBN powder was subsequently nitrided at 900 °C in flowing NH_3 gas with a flow rate of 1000 ml/min for 4 h. The furnace was allowed to cool down to room temperature in the flow of N_2 gas.

Using the same conditions, but without the presence of cBN, TiO_2 nanoparticles were synthesized. These powders, after the sol–gel solution, were subjected to calcination in air atmosphere at temperatures of 250 °C, 400 °C, 600 °C, 700 °C for 2 h each. They were then nitrided in flowing NH_3 gas for 4 h.

2.2. Characterization of the coated powders

The morphology of the powders after coating was analyzed by the scanning electron microscope (SEM; XL30SFEG, Philips). Thickness of the coated layer, TiN powder size and the interface between TiN and cBN particles was observed by transmission electron microscope (TEM; Tecnai G2 F30, FEI) with electron diffraction and energy

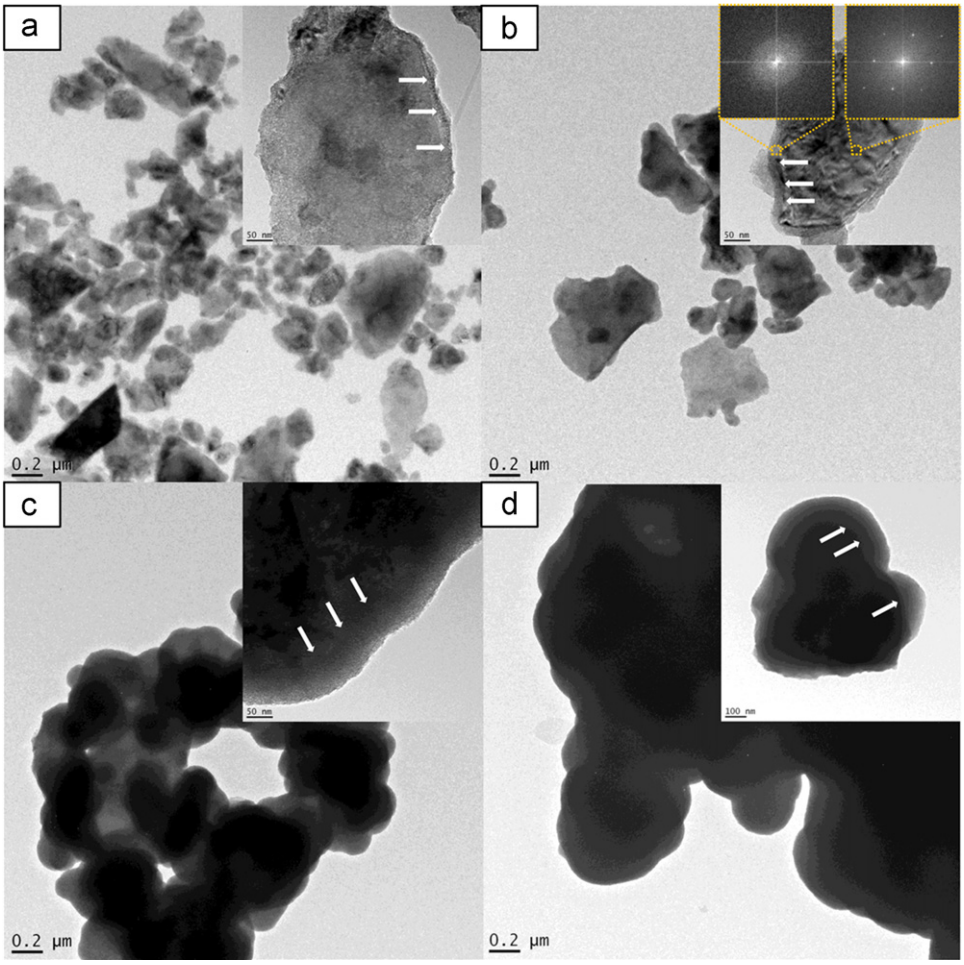

Fig. 2. TEM images of TiO_x coated cBN particles with (a) 0.71, (b) 1.42, (c) 2.85 and (d) 4.30 ml TTIP used. The diffused ring obtained by using the Fourier transform image obtained from the lattice image in (b) shows the lack of a crystal structure of the coated layer.

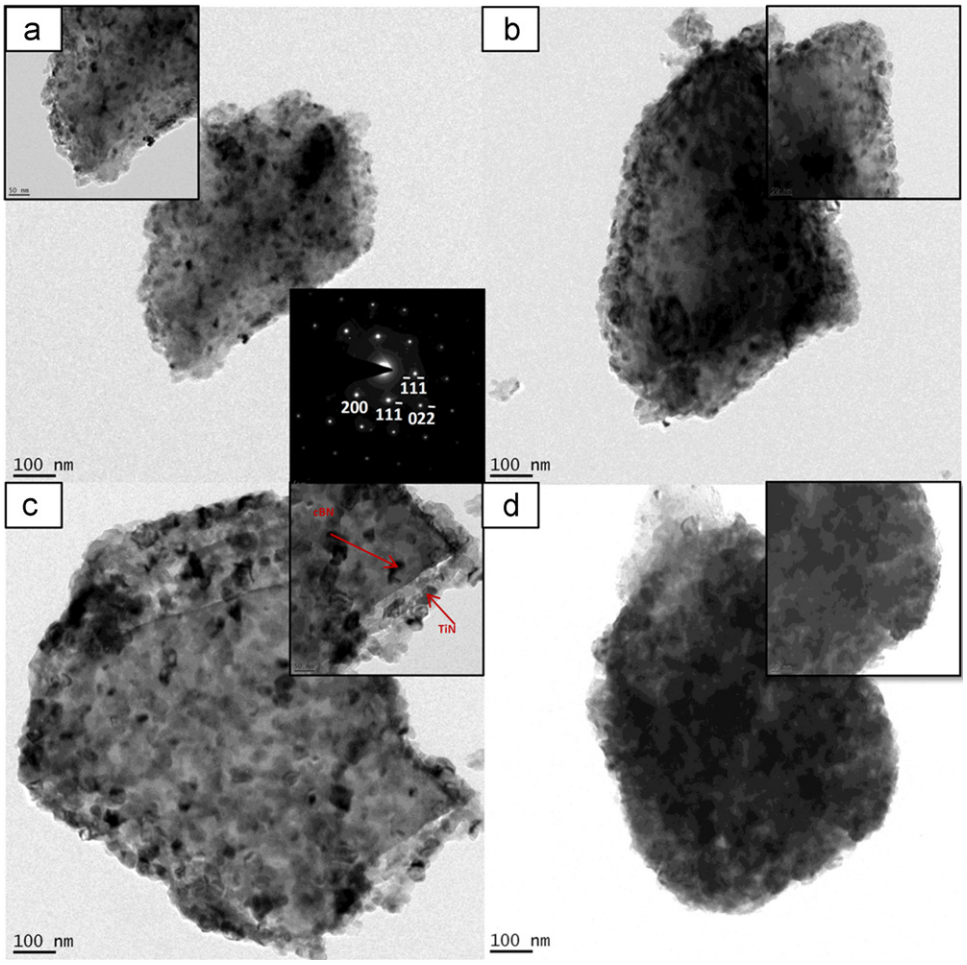

Fig. 3. TEM images of nanosized TiN coated cBN particles. Fraction of TiN was calculated to be: (a) 10 vol%, (b) 20 vol%, (c) 40 vol% and (d) 60 vol% TiN. The spot patterns of cBN were superimposed with the rings pertaining to TiN.

dispersive X-ray analysis (EDS). Phase compositions of the powders were identified by X-ray diffraction (XRD; D/MAX IIIC, Rigaku). TGA (Setsys 16/18, Setaram) and DCS (DSC 404 C, Netzsch) analysis tests of the sol–gel coated powders were carried out in air atmosphere up to 1000 °C at 5 °C/min.

3. Results and discussion

3.1. Preparation of TiO_x coated cBN particles

The hydrolysis (Eq. (1)) and polycondensation (Eqs. (2) and (3)) of the titanium alkoxide proceed according to the following reactions [13]:

$$\text{Ti–OR} + \text{H}_2\text{O} \rightarrow \text{Ti–OH} + \text{R–OH} \quad (1)$$

$$\text{Ti–OH} + \text{M–OR} \rightarrow \text{Ti–O–Ti} + \text{ROH} \quad (2)$$

The reaction stops with the inclusion of two water molecules:

$$\text{Ti–OH} + \text{Ti–OH} \rightarrow \text{Ti–O–Ti} + \text{H}_2\text{O} \quad (3)$$

where R is the alkyl group. The above reactions govern the transformation of the precursor material into the oxide network. Therefore, these reactions play an important role in the structure and morphology of the resulting oxide. Their roles can be optimized if the experimental conditions are carefully adjusted. Transition metal alkoxides are well known for their high reactivity towards water [14]. To obtain a fine coated layer on the surface of cBN particles, fast hydrolysis of the TTIP should be prevented. This can be achieved by using water in fairly dilute concentrations. Upon mixing, hydrolysis of the TTIP occurs giving fine nuclei of titania that grow during the condensation process. Since the concentration of water in our experiments was kept very low, hydrolysis can be assumed to commence at fairly low rates. Due to the presence of cBN particles in the solution, a heterogeneous nucleation of TTIP takes place on the surface of cBN particles forming a thin coated layer of titania. Fig. 2 shows the TEM image of uniformly coated single cBN particles with different amounts of TTIP used. As seen in the figure, the coated layer homogenously covers the entire cBN particles. The arrows in the figures point to the interface between the coated layer and the cBN surface. Typically, sol–gel derived products are amorphous in nature, requiring further heat treatment. Selected area diffraction pattern obtained in the region of coated layer shows a diffused ring in Fig. 2b, confirming the amorphous nature of the layer. It was observed that an increase in the amount of alkoxide used in the experiment resulted in an increase in the thickness of the coated layer. Coating layers that resulted in using the lowest amounts of TTIP as seen in Table 1, had the lowest average value of the coating layer thickness which was under 10 nm while the thickest coated layers ranged over 50 nm. Aggregated particles were observed in the samples that contained high values of TTIP used (0.0094 and 0.014 moles TTIP). This problem of aggregation can be minimized by using relatively lower values of TTIP/cBN. The particles in sample 2 suggested optimum conditions as they were well dispersed and had a reasonably thick coated layer.

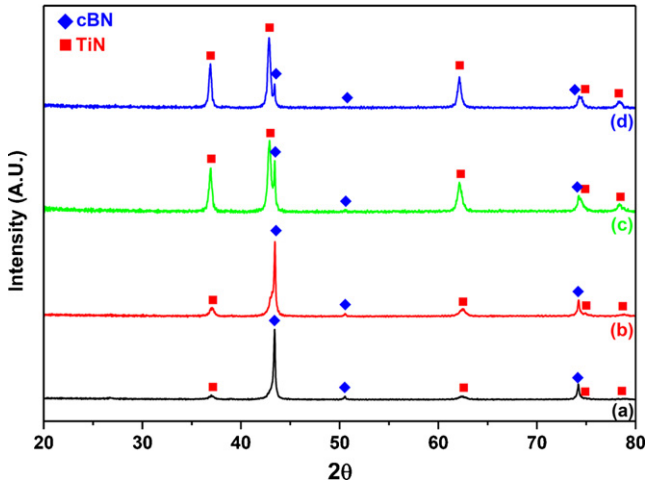

Fig. 4. XRD patterns of the TiN coated cBN powder. The intensity of TiN peaks increased from (a) to (d) as a function of the amount of precursor used.

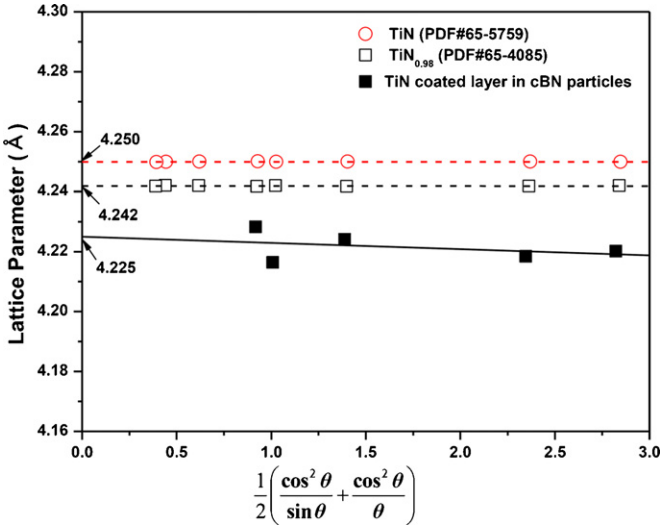

Fig. 6. The lattice constant of 20 vol% coated TiN measured by extrapolation from Nelson–Riley equation.

3.2. Preparation of TiN coated cBN particles

The nitridation process of the sol–gel derived coated layer of TiO_x may proceed with the reaction shown below [15]:

$$NH_3 \rightarrow (1/2)N_2 + (3/2)H_2 \quad (4)$$

$$2TiO_2 + H_2 \rightarrow Ti_2O_3 + H_2O \quad (5)$$

$$TiO_2 + H_2 \rightarrow TiO + H_2O \quad (6)$$

$$Ti_2O_3 + NH_3 \rightarrow 2TiN + 3H_2O \quad (7)$$

$$2TiO + 2NH_3 \rightarrow 2TiN + 2H_2O + H_2 \quad (8)$$

As seen in Fig. 3, the nitridation process yields nanocrystalline TiN coated cBN particles. The amorphous layer of Titania is transformed into TiN particles of the nanometer scale after NH_3 treatment. The TiN nanoparticles are uniform in size and shape and are homogenously distributed on the surface of cBN. Weak rings pertaining to f.c.c. TiN phase had been identified to coexist with the spot patterns for cBN by the power spectrum obtained from the selected area electron diffraction (SAED). Smallest TiN particles ranged to approximately 10 nm in diameter. However, the largest diameter of TiN nanoparticles was estimated to be around 45 nm, corresponding to sample 4 (Fig. 3d).

The XRD patterns in Fig. 4 reveal the phase compositions of the coated cBN powder samples. No peaks other than those corresponding to cBN and TiN could be observed in all samples. It was noted that the TiN peak intensity increased with increasing initial TTIP content used. A relationship of TiN particle size with the TiO_x coating layer thickness is shown in Fig. 5. It can be seen that the size of TiN particles is directly dependent upon the thickness of initial coating layer. Coating layers with smallest values of thickness gave TiN particles with an average size of 15 nm while the largest TiN particle sizes obtained were around 45 nm. An increase in reagent concentration causes the reaction rates to increase. Hence, with higher TiO_x concentration (as coating layer thickness), the conversion to TiN is accelerated leading to larger TiN particles. The lattice constant of TiN, measured by extrapolation from Nelson–Riley equation [16] in Fig. 6, was 4.225 Å, which is smaller than the value of pure TiN (a_0 = 4.250 Å) [17], indicating that the TiN contains a small amount of oxygen. It was confirmed by elemental analysis that around 3 wt% oxygen was present in the TiN coated cBN powders. The f.c.c. TiN_x phase is chemically stable over a wide stoichiometric composition ($0.5 \leq x \leq 1.2$). In substoichiometric TiN_{1-x}, the most significant defect is the nitrogen vacancy and in nitrogen-rich TiN_{1+x} excess nitrogen behaves like an interstitial

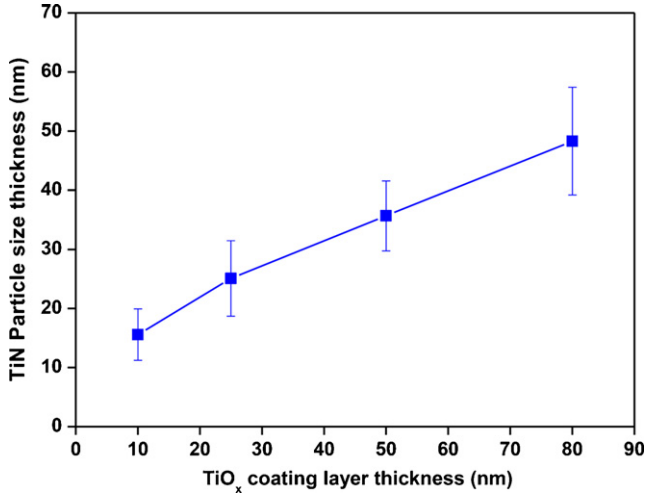

Fig. 5. Relationship showing the average size of TiN particles increases as the thickness of TiO_x coating layer increases.

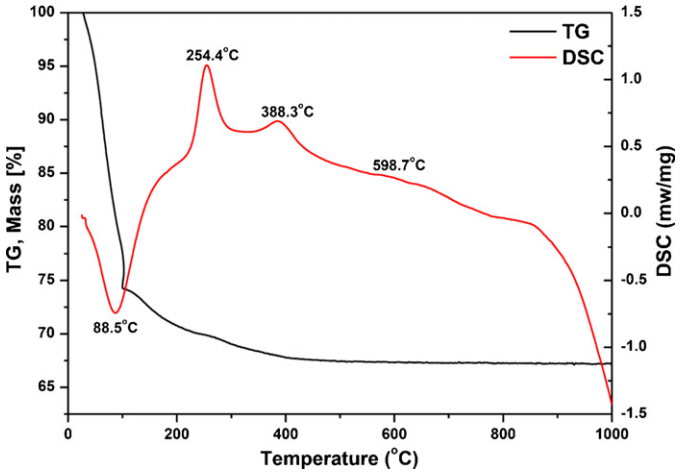

Fig. 7. DSC/TGA curves of the sol–gel prepared coated cBN particles showing the crystallization behavior of TiO_2.

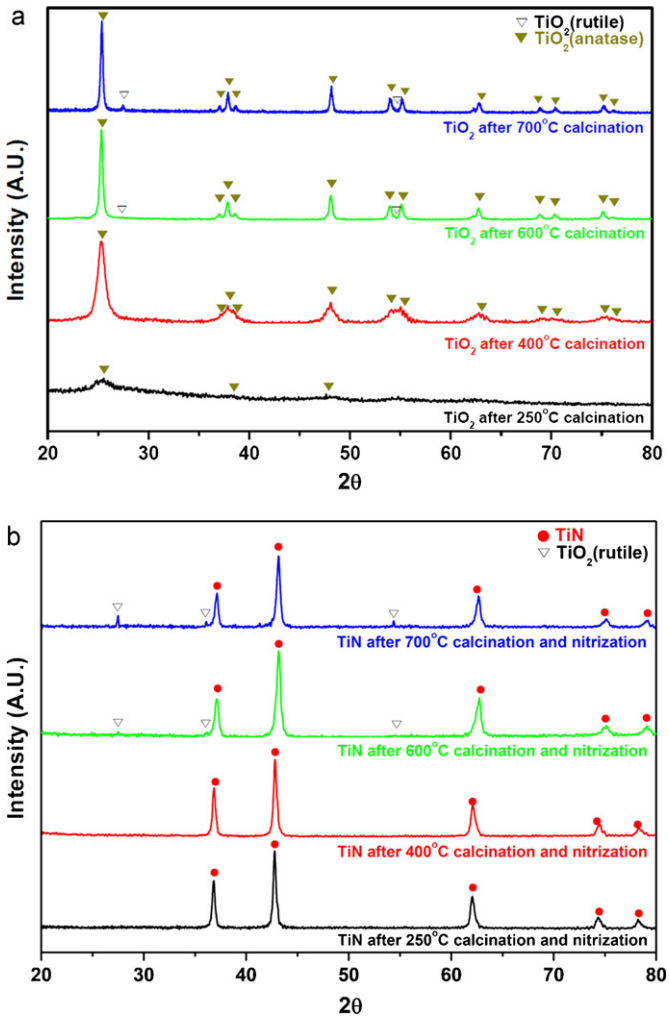

Fig. 8. XRD curves of the (a) calcined and (b) nitrided TiO_2 nanoparticles at 900 °C. Crystallinity of the Anatase phase increases with calcination temperature while very small peaks of rutile were observed after 600 °C.

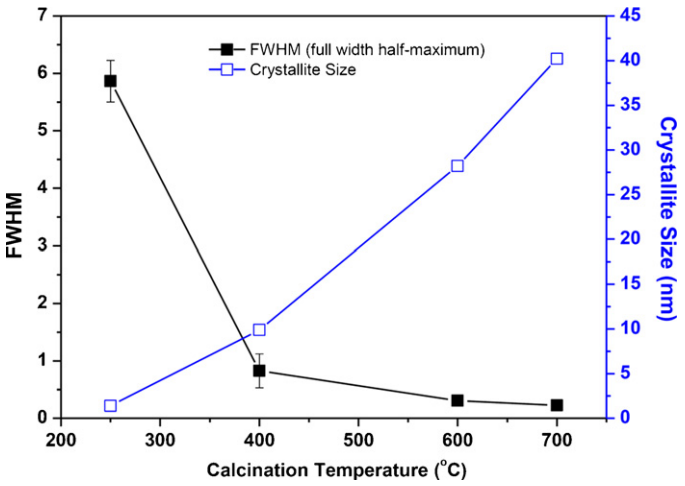

Fig. 9. Crystallite sizes of the TiO_2 nanoparticles, calculated by Full width half maximum method, were seen to increase with the calcination temperature.

defect [18]. Due to the strong affinity of oxygen with regard to the titanium and the ability of TiN to contain high concentration of point defects, a minute fraction of oxygen atoms may still remain in the TiN lattice after nitridation.

The DSC and TG curves in Fig. 7 show the crystallization behavior of TiO_2 in air atmosphere. The first stage of mass loss in the TG curve can be described as the evaporation of water, which is roughly until 100 °C. Decomposition of residual organic precursor material takes place, which can be characterized by the second stage of mass loss until 400 °C. No further mass loss could be observed in the last stage from 400 to 1000 °C. It was seen that crystallization of the anatase phase of TiO_2 was marked by the exothermic peak obtained at 388 °C in the DSC curve. Conversion of anatase to rutile phase occurred at roughly 600 °C, as shown by the second and smaller exothermic peak at 598 °C.

TiO_2 nanoparticles were separately synthesized without the presence of cBN particles, using the same conditions. Fig. 8a shows the crystallization behavior of the nanoparticles with different calcination temperatures. The presence of very weak peaks of Anatase phase of TiO_2 could be observed, even in the powder calcined at 250 °C, which was otherwise amorphous in nature. The crystallinity of the TiO_2 particles grew with an increase in calcination temperature. This was confirmed by a gradual increase of intensity and a sharpening of peaks. Some peaks corresponding to the rutile phase were observed in the samples calcined at 700 °C.

From Fig. 8b, it was observed that the samples that were calcined at 250 °C and 400 °C had converted completely to TiN after NH_3 treatment. No TiO_2 peaks could be seen in the XRD results for these samples. However, samples that were calcined at 600 °C and 700 °C contained a fraction of retained TiO_2 of the rutile phase only. From these results, it could be inferred that only the anatase phase of TiO_2 could be converted to TiN and amorphous titania would be best suited for nitridation to obtain highly pure TiN.

Crystallite sizes of the TiO_2 nanoparticles were calculated from the Scherrer's equation:

$$L = \frac{K\lambda}{\beta \cos \theta} \tag{9}$$

where λ is the wavelength of the X-ray radiation (CuKα = 0.15406), K is a constant of value 0.89, β is the line width at half maximum height, and θ is the diffraction angle. The crystallite sizes were seen to increase with increasing calcination temperature (Fig. 9).

4. Conclusions

Considering the results that were obtained, a mechanism of coating cBN particles by the sol–gel reaction can now be described. TTIP drops are hydrolyzed upon entering the parent solution that contains water and cBN particles. The presence of cBN particles makes it easier for the Ti–OH to nucleate on their surface due to a reduced energy of nucleation. The rate of hydrolysis of TTIP is dependent upon the alkoxide: water ratio and is kept relatively slow by the lower amount of water present in the solution. The conditions reported in this paper were favorable to coat cBN particles with a smooth coating layer of titanium oxide, which was amorphous in nature. The coating layer on the cBN was converted to fine TiN particles upon a thermal treatment in NH_3 gas. It was observed that an increase in the coated layer thickness accounted for an increase in the amount and the size of the coated nano TiN particles, with particle sizes ranging from 10 nm to roughly 45 nm. Titanium oxide that was calcinated at 600 °C or above did not completely transform to TiN. The retained titanium oxide was identified as rutile.

Acknowledgements

This research was supported by NSL (National Space Lab) program through the Korea Science and Engineering Foundation funded by the Ministry of Education, Science and Technology (N01110292).

References

[1] Cubic Boron Nitride: Handbook of Properties, General Electric CRD Report No. 72CRD178, 1972.
[2] R. Reidel, Handbook of Ceramic Hard Materials, Wiley-VCH, 2000.
[3] J. Barry, G. Byrne, Wear 247 (2001) 152–160.
[4] M.A. Yallese, K. Chaoui, N. Zeghib, L. Boulanouar, J.F. Rigal, J. Mater. Process. Technol. 209 (2009) 1092–1104.
[5] Y.S. Liao, H.M. Lin, J.H. Wang, J. Mater. Process. Technol. 201 (2008) 460–465.
[6] E.O. Ezugwu, R.B. Da Silva, J. Bonney, A.R. Machado, Int. J. Mach. Tool Manuf. (2005) 1009–1014.
[7] Z.G. Wang, M. Rahman, Y.S. Wong, Wear 258 (2005) 752–758.
[8] E. Benko, J.S. Stanisław, B. Krolicka, A. Wyczesany, T.L. Barr, Diam. Rel. Mater. (1999) 1838–1846.
[9] J. Angseryd, M. Elfwin, E. Olsso, H.O. Andren, Int. J. Refract. Met. (2008).
[10] P. Klimczyk, E. Benko, K.L. Jablonska, E. Piskorska, M. Heinonen, A. Ormaniec, W.G. Zawislan, V.S. Urbanovich, J. Alloy Comp. (2004) 195–205.
[11] M.A. Davies, Y. Chou, C.J. Evans, Ann. CIRP 45 (1996) 77–82.
[12] H. Yoshida, S. Kume, J. Mater. Res. 12 (1997) 585–588.
[13] A.C. Pierre, Introduction to Sol–Gel Processing, Kluwer, 1998.
[14] E.A. Barringer, H.K. Bowen, Langmuir 1 (1985) 414–420.
[15] K. Kamiya, T. Yoko, M. Bessho, J. Mater. Sci. 22 (1987) 937–941.
[16] B.D. Cullity, Elements of X-ray Diffraction, Addison-Wesley, 1978.
[17] Powder Diffraction File 65-5759, International Centre for Diffraction Data, Newtown Square, PA.
[18] P.E. Schmid, M.S. Sunaga, F. Levy, J. Vac. Sci. Technol. A 16 (1998) 2870–2875.